

# COMPUTED SPECKLE DECORRELATION (CSD) AND ITS APPLICATION FOR FATIGUE DAMAGE MONITORING

J. Scott Steckenrider  
James W. Wagner

The Johns Hopkins University  
Center for Nondestructive Evaluation  
102 Maryland Hall  
Baltimore, MD 21218

## INTRODUCTION

A video-based laser speckle technique has been developed for non-contact surface deformation analysis and mapping at speeds approaching video frame rates. This technique, Computed Speckle Decorrelation (CSD), makes use of the speckle decorrelation associated with surface deformation. In its current application, CSD is a method of full field inspection which has been used both to locate fatigue damage sites and to measure damage severity during fatigue deformation in reverse bending fatigue of a cylindrically notched aluminum specimen. With the development of the CSD method it will now be possible to examine in greater detail the progression of fatigue damage in thick graphite/epoxy composite materials, allowing a much faster and much more quantitative analysis than was previously available through film based techniques[1].

The uses of laser speckle photography are widespread in mechanics and metrology[2][3]. Most of the applications of traditional laser speckle involve the comparison of two correlated speckle patterns of a given field before and after some perturbation to the system has occurred. From the relative displacement of the correlated patterns, either Young's fringes or isothetic fringes, which quantitatively determine the speckle spacing, and thereby displacement and displacement gradient (strain) information, may be produced when the information recorded on the specklegram is processed[4]. If the displacement, displacement gradient, surface tilt, or surface out-of-plane displacement is excessive, or if the surface morphology changes, the correlation of the speckle patterns is reduced or may be lost so that the fringes may become distorted or lose visibility altogether. In this latter case the speckle patterns are said to be decorrelated and accurate quantitative information about in-plane surface displacement is no longer available. However, the regions over which speckle correlation is lost have been shown to correspond to areas of plastic deformation in alloys and, as such, have been used to study plastic zone growth during fracture of aluminum and steel alloys[5].

The laser speckle decorrelation technique is now being used to monitor for fatigue damage in thick composite materials[6]. To evaluate properly damage to specimens under cyclic loading, the inspection system must be capable of showing both instantaneous changes in the condition of the specimen as well as keep track of cumulative degradation. The feasibility of using the speckle decorrelation method simply to map cumulative damage has been established using quasi-static deformation and paused fatigue testing. Unlike the previous work in the fracture of alloys, however, deformation localization alone is insufficient to provide a complete analysis of the fatigue process. A new technique is therefore required which will provide both quantitative decorrelation information, and provide it in real time.

A more recent application of traditional laser speckle interferometry, Computer Speckle Interferometry (CSI), overcomes one of those two obstacles by incorporating video methods to speed processing time[7]. Computed Speckle Decorrelation (CSD) now combines earlier speckle decorrelation work with this newer computer based technique to achieve a method which not only discerns regions of deformation, but also provides a quantitative measurement of the degree of deformation at each image location. In addition, it provides this information far more quickly than traditional film based systems, with speeds potentially approaching video frame rates.

Examined in this study was the application of CSD to monitor for fatigue degradation of a specimen of 2024-T4 aluminum subjected to reverse bending fatigue. The specimen was cut with symmetrically located cylindrical notches, and the decorrelation of the specimen surface between the notches on the un-notched side was monitored as a function of fatigue cycle number.

## LASER SPECKLE DECORRELATION

Recall that laser speckle is the complex interference pattern that results when a coherent source (e.g. a laser) illuminates an optically rough surface, one on which the microscopic perturbations of the surface are on the order of or greater than the wavelength of the illuminating light[8][9][10]. The resulting speckle patterns are unique to the surface from which they are derived, and as that surface changes, so will its speckle pattern change. One may therefore use speckle photography, where two speckle fields corresponding to the initial and altered states of an object are recorded (usually on photographic film), to store or transfer information about the surface's change. This information can then be extracted by Fourier filtering the specklegram[11][12].

### Effect of surface change on speckle pattern

There are three distinctive ways in which the speckle pattern can change owing to alterations of an imaged surface. These are in-plane displacement, in-plane displacement gradient, and morphological change of the pattern. Traditional laser speckle interferometry analyzes and maps the first two, but it is the third that is of interest in this work. The imaged surface may have undergone one of several transformations in order to produce this speckle morphology change: excessive surface displacement (either in-plane, out-of-plane, or rotational), excessive elastic strain (possibly inducing Poisson contraction), excessive surface tilt, or by plastic deformation of the surface.

## Optical filtering for decorrelation of speckle interferograms

The most commonly used method of extracting information from correlated speckle interferograms is that of pointwise spatial filtering. In this case, the interferogram is scanned and interrogated by a very narrow collimated beam (i.e. a raw laser beam), and a screen is placed at a distance sufficiently large to satisfy Fraunhofer diffraction conditions. The matched speckle pairs will act as coherent pairs which give rise in the diffraction plane to Young's fringes, perpendicular to the displacement vector. If all of the speckle are separated by the same vector their Young's fringes would be coincident, and these fringes would be separated by a vector related to the speckle separation. If the speckle pairs are separated by substantially different vectors, or if the morphology has changed so that matching pairs no longer exist, the screen will show only a diffraction halo, and no fringes will be visible[13].

As described in Ref. [4], the Young's fringe contrast is proportional to a normalized cross correlation function of the initial and final states of the speckle field pattern. For most experimental methods, surface tilt, displacement, and defocus can be controlled so that their effects on decorrelation are insignificant. Decorrelation will be dominated therefore by changes in surface morphology, which result from surface deformation. It is this effect which was used to delineate regions of fatigue damage.

## Computed decorrelation

The film based decorrelation method described above can be quantified to some extent by comparing the contrast of Young's fringes at each location, but factors such as filtering beam illumination area and secondary speckle would still contribute an error to any measurement. There is however no way of speeding the development and analysis process in film. Therefore CSD appears to be a good solution, allowing the computational determination of an exact correlation value while eliminating the cumbersome film development and pointwise analysis processes.

In order to apply video techniques, the imaging system must have a large enough f-number to produce speckle larger than the element size of the CCD imaging array, to avoid the error caused by speckle averaging, but not too large, in order to maintain high resolution. Once the camera and image acquisition system is set, a reference speckle image is digitized and stored to computer memory. The 512x464 image is analyzed in 810 discrete 16x16 pixel subsets, neglecting the outer 16 pixel boundary (to allow for rigid body motion as explained below), yielding a 30x27 reduced correlation image. The correlation of each subset is computed using the expression for correlation  $\mathfrak{R}_c$ , given as

$$\mathfrak{R}_c\{a(x,y), b(x,y)\} = \mathcal{F}^{-1}\{A(\omega, \phi) \times B^*(\omega, \phi)\} \quad (1a)$$

where

$$A(\omega, \phi) = \mathcal{F}\{a(x,y)\}, \quad (1b)$$

$$B(\omega, \phi) = \mathcal{F}\{b(x, y)\}, \quad (1c)$$

$a(x, y)$  and  $b(x, y)$  represent the "before" and "after" image intensity fields being correlated,  $\mathcal{F}$  is the Fourier transform, and  $B^*$  is the complex conjugate of  $B$ . The amplitude of the correlation peak, which is located at the center of motion between  $a(x, y)$  and  $b(x, y)$  (0,0 for no motion), is normalized by subtracting the average amplitude of the uncorrelated background then dividing by that background, giving the normalized correlation factor

$$CF(n, m) = \frac{(\mathfrak{R}_c^{peak} - \mathfrak{R}_c^{avg})}{\mathfrak{R}_c^{avg}}. \quad (2)$$

where  $n$  and  $m$  are the indices of the 16x16 subsets.

Owing to the finite number of speckle within each subset, and the potential non-uniformity of illumination, the integrated intensity in each subset will not be the same, and therefore the  $CF(n, m)$  will vary from subset to subset even when the two images are perfectly correlated (i.e. during autocorrelation). As a result, a reference  $CF^{auto}(n, m)$  generated by correlating the reference image with itself, must be kept for each subset. Subsequent  $CF(n, m)$ 's are then normalized by the reference  $CF^{auto}(n, m)$  which should result in a final correlation value of exactly 1.0 for an unchanged speckle pattern, and drop off toward 0.0 as the speckle pattern decorrelates.

The other potential difficulty in this technique is the partial decorrelation which occurs when the two images have been slightly displaced relative to one another. This contribution to decorrelation is essentially the same as that mentioned above for the film based speckle technique where the illumination area of the laser beam is finite and any motion of the images causes a reduction in "common area" between the two interfering speckle patterns. The computer based technique is able to deal with this problem quite simply by shifting the one of the images in computer memory to remove this motion. The images can then be correlated as before in 16x16 subsets. However, if motion occurs, the outer 16x16 subsets would still be slightly decorrelated by the motion itself, and they are therefore not analyzed.

## EXPERIMENTAL ARRANGEMENT

Figure 1 is a drawing of the experimental fatigue fixture showing the 2024-T4 aluminum test specimen. The specimen was 30 cm in length, 3.33 cm wide, and 1.25 cm thick, with a 0.5 cm radius cylindrical groove cut through the thickness on opposing sides. The specimen was clamped as shown, where the fixed end was clamped 3.2 cm from the notch centers, and the last 2.75 cm of the other end was held in the deflection arm. The bar was illuminated from above by a 20 mW He-Ne laser inclined at an angle of approximately 30 degrees with the specimen normal. The camera used was a Pulnix 540 with a Nikon 1:1 macro lens set for 0.3x magnification and was also mounted above the specimen looking normal to its surface. For this system, an f-number of 32 was used. This would give a speckle size of 25  $\mu\text{m}$ , and with a CCD element size on the camera of 15.5  $\mu\text{m}$ , we had an

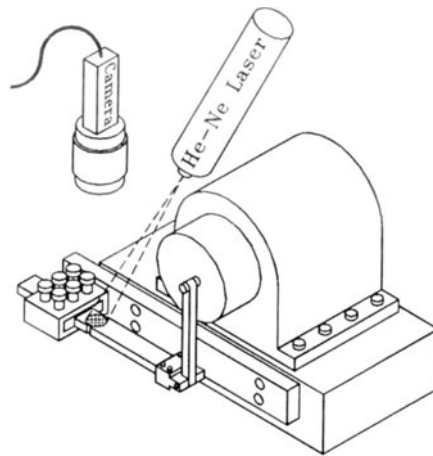


Figure 1. Diagram of experimental fatigue fixture and specimen.

average of at least 2.5 pixels per speckle. Once the system was prepared and in place, a reference image was taken and the correlation process was begun.

While a 386 20MHz computer processed the autocorrelation of the reference image, the specimen was cycled with an end deflection of  $\pm 0.95$  cm for 1000 cycles at 28.75 Hz and returned by visual alignment to its zero position. The second image was then digitized, and while that correlation was in progress (each image correlation took approximately 4 minutes), the specimen was cycled for another 1000 cycles. This process was repeated until the total number of cycles reached 20,000, at which point the 20,000 cycle image was also written to computer memory. The specimen was cycled an additional 2000 cycles, and two correlations were performed comparing the 22,000 cycle image to the initial 0 cycle image and the 20,000 cycle image. This provided both cumulative (22,000 vs. 0 cycles) and incremental (22,000 vs. 20,000 cycles) damage information. Next, three consecutive images were digitized at 22,000 cycles and correlated with the 20,000 cycle image, each time after visually resetting the rotating drum to its zero position, to determine the effect of error in drum alignment for each image. Finally, two consecutive images were digitized with no changes to the specimen between them to determine the effect of camera noise.

## RESULTS AND DISCUSSION

Figure 2 shows the raw images corresponding to 0 and 22,000 cycles, as well as the plot of their correlation. Although no specific region of decorrelation is directly evident in the raw images themselves, the damage is easily seen in the resulting correlation plot. Figure 3 shows the progression of these damage zones through 22,000 cycles. The specimen outline is illustrated to show the location of the notches. As would be expected, the damage zones are relatively symmetric, and gradually grow from the notch tips as the specimen is cycled. Figure 4 shows the correlation plot generated by the final two consecutive images with no cycling between them and illustrates the contribution of camera noise to decorrelation. The minimum correlation is approximately 0.9, which represents a decorrelation of

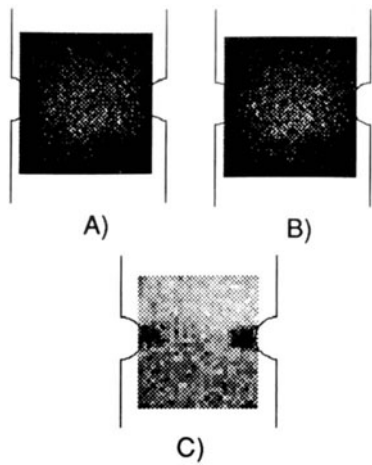


Figure 2. Comparison of images A) at 0 cycles, B) after 22,000 cycles, and C) correlation between a and b.

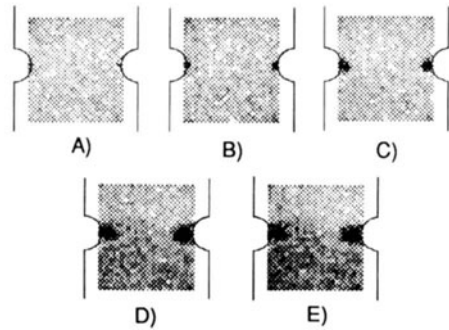


Figure 3. Correlation plots after fatiguing for A) 2,000 cycles, B) 4,000 cycles, C) 10,000 cycles, D) 20,000 cycles, and E) 22,000 cycles.

10%. This error could be corrected or at least minimized by running a separate sync signal from the camera to the computer and/or by applying frame-averaging algorithms. Finally, Fig. 5 shows a comparison of correlation plots of three attempts to "zero" the rotating fatigue drum at 22,000 cycles, as correlated with the 20,000 cycle image.

Two things are evident. First, Fig. 5 shows that the instantaneous decorrelation occurs only at the tip of the damage zone, and that the material which was deformed in cycles 0-20,000 remains essentially unchanged in cycles

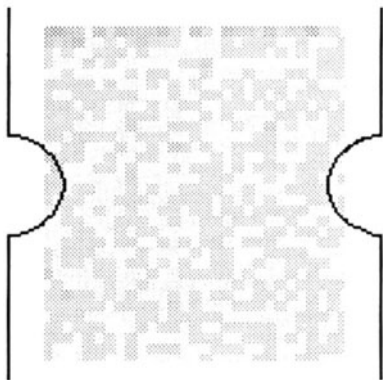


Figure 4. Plot of decorrelation contributed by camera noise.

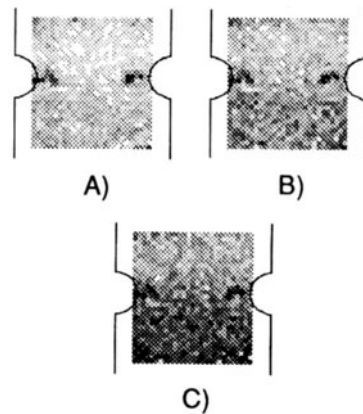


Figure 5. Correlation plots of three attempts to "zero" the rotating fatigue drum.

20,000-22,000. Microscopic evaluation revealed a fatigue crack in the specimen with its tip located at the center of this instantaneous decorrelation zone. Second, these plots show the error associated with slight misalignment of the drum to be up to 20%, but that this error occurs only on the deflected side of the specimen, as would be expected. This error could be corrected by altering the reverse bending machine to include a "keyed" zero position, but such action was not feasible during this work.

## CONCLUSIONS

Computed Speckle Decorrelation has been shown to be an effective tool for monitoring for incremental and cumulative fatigue damage. Localized regions of damage were indicated at the tips of the specimens' notches, and the size of those damaged regions was shown to increase with the number of cycles. The technique also demonstrated the ability to discern instantaneous damage accumulation, indicating that previously deformed regions were relatively unchanged in subsequent fatigue cycles.

Three minor improvements in the technique were indicated as necessary. First, although the speed of this method is much greater than that of any film based technique, substantial improvements could and will be made by performing most if not all of the correlation algorithm in hardware through the addition of a DSP board to the system, rather than in software, allowing for analysis approaching real time. Second, camera noise could be reduced markedly by improving the synchronization of the camera-computer interface and/or by performing some degree of frame-averaging at the image acquisition stage, although frame-averaging would likely reduce the speed somewhat. Finally, for the system to be used to its optimum capability, the object of analysis should either not move at all or at least be returned to its reference position with greater accuracy than was possible in the studies presented here (ideally to within less than a wavelength of the illuminating light).

Several potential applications exist for which this technique appears well suited. For localized corrosion processes, CSD would be able to determine *in situ* regions of corrosion, requiring only visual access to the corroding surface. For wear studies, CSD would be able to localize and, to some degree, quantify the worn areas of any rough surface so long as the surface could be returned to some reference position after wear with the accuracy given above. For the study of impact damage, CSD could localize the surface plastic zone around the impact, and possibly even determine the distribution of the degree of damage in that zone, again if the specimen could be impacted in the same position as it was analyzed.

## ACKNOWLEDGEMENT

The authors would like to acknowledge the funding granted them by The Defence Advanced Research Projects Agency.

## REFERENCES

1. A more detailed description of this work has been presented in "Computed Speckle Decorrelation (CSD) for the study of fatigue damage", submitted for publication to *Optics and Lasers in Engineering*.
2. Erf, R.K., (ed.), "Speckle Metrology." Academic Press, New York, 1978.

3. Francon, M., "Laser Speckle and Applications in Optics." Academic Press, New York, 1979.
4. Yamaguchi, I., Fringe formation in speckle photography, *J. Opt. Soc. Am. A*, 1 (1), 1984, 81-86.
5. Steckenrider, J.S. and Wagner, J.W., Laser Speckle Decorrelation as a Non-Contact Method for Brittle-Ductile Fracture Differentiation, *Exp. Mech.*, 31 (1), 1991, pp. 8-13.
6. Steckenrider, J.S. and Wagner, J.W., Laser speckle correlation studies of compression-compression fatigue damage in thick composites, *Nondestructive Evaluation (NDE) and Materials Properties of Advanced Materials - Proceedings 1991*, The Minerals, Metals, and Materials Society, Feb. 1991.
7. Chen, D.J. and Chiang, F.P., Computer Speckle Interferometry (CSI), *Hologram Interferometry and Speckle Metrology - Proceedings 1990*, Society for Experimental Mechanics, Nov. 1990.
8. Dainty, J.C. (ed.), "Laser Speckle and Related Phenomena." Springer-Verlag, New York, 1975.
9. Jenkins, F.A. and White, H.E., "Fundamentals of Optics" Second Edition, McGraw-Hill, New York, 1950.
10. Hecht, E., "Optics" Second Edition, Addison-Wesley Publishing, Reading, Massachusetts, 1987.
11. Chen, J.B. and Chiang, F.P., Statistical Analysis of Whole-field Filtering of Specklegram and Its Upper Limit of Measurement, *J. Opt. Soc. Am. A*, 1 (8), 1984, 845-849.
12. Li, D.W., Chen, J.B. and Chiang, F.P., Statistical Analysis of One-beam Subjective Laser-speckle Interferometry, *J. Opt. Soc. Am. A*, 2 (5), 1985, 657-666.
13. Jones, R. and Wykes, C., "Holographic and Speckle Interferometry." Second Edition, Cambridge University Press, Cambridge and New York, 1989.